Available online at www.sciencedirect.com

SCIENCE DIRECT®

ELSEVIER

International Journal of Mass Spectrometry 239 (2004) 7–16

International Journal of Mass Spectrometry

www.elsevier.com/locate/ijms

A selected ion flow tube study of the reactions of H_3O^+, NO^+ and $O_2{}^+$ with some monoterpene oxidation products

N. Schoon[a,*], C. Amelynck[a], L. Vereecken[b], H. Coeckelberghs[b], E. Arijs[a]

[a] *Belgian Institute for Space Aeronomy, Ringlaan 3, B-1180 Brussels, Belgium*
[b] *Department of Chemistry, University of Leuven, Celestijnenlaan 200F, B-3001 Heverlee, Belgium*

Received 13 July 2004; accepted 2 September 2004
Available online 8 October 2004

Abstract

We have studied the reactions of H_3O^+, NO^+ and $O_2{}^+$ with five oxidation products of monoterpenes: pinonaldehyde (oxidation product of α-pinene), nopinone (β-pinene), α-pinene oxide (α-pinene), 4-acetyl-1-methylcyclohexene (d-limonene) and caronaldehyde (Δ^3-carene).

It was found that all reactions studied proceed with a rate constant close to the collision rate constant, calculated with the parameterized equation of Su and Chesnavich. The dipole moment and polarizability of the neutral reactants, needed for the calculation of these collision rate constants, were determined by quantum chemical calculations.

Analysis of the ion product spectra shows that H_3O^+ reacts with 4-acetyl-1-methylcyclohexene and nopinone by non-dissociative proton transfer. The major channel of the reaction of H_3O^+ with α-pinene oxide, pinonaldehyde and caronaldehyde is elimination of a water molecule following protonation.

The reaction of NO^+ with 4-acetyl-1-methylcyclohexene and nopinone is mainly determined by charge transfer. Charge transfer is also observed in the reaction of NO^+ with α-pinene oxide, pinonaldehyde and caronaldehyde, as well as a series of fragment ions. A non-negligible hydride ion transfer channel also occurs in the product spectra of NO^+ with pinonaldehyde. For the NO^+–nopinone and NO^+–caronaldehyde reaction also three-body association is observed.

The product spectra of $O_2{}^+$ with the neutral reactants show multiple products, mainly characterized by charge transfer and fragmentation, and are less suited to be used for CIMS detection of the monoterpene oxidation products.

Keywords: SIFT; Ion–molecule reaction; Monoterpenes; Proton transfer; Charge transfer; Hydride ion transfer

---

1. Introduction

It is well established that vegetation is emitting an amount of non-methane volatile organic compounds (BVOC's) into the atmosphere, which exceeds largely emissions of anthropogenic origin [1,2]. A considerable fraction of those BVOC's are $C_{10}H_{16}$ monoterpenes [3–5], the global emission of which has been estimated to be 127 MT per year [6].

The oxidation of monoterpenes in the atmosphere, initiated by reaction with ozone, OH and NO_3 radicals, leads to a variety of products, some of which play an important role in atmospheric chemistry [7]. A number of those oxidation products are very condensable and contribute by gas to particle conversion to the formation of the so-called secondary organic aerosols [8], which can have an impact on the climate and the local radiation budget. An understanding of the monoterpene oxidation mechanism is, therefore, crucial in tropospheric chemistry.

The oxidation products of monoterpenes have been quantified in the laboratory by different techniques such as, gas chromatography with flame ionization detection (GC–FID) [9], collection of gas samples on solid absorbent (Tenax-GC) followed by analysis through GC–FID [10–15],

---

[*] Corresponding author. Tel.: +32 2373 0391; fax: +32 2374 8423.
E-mail address: Niels.Schoon@bira-iasb.oma.be (N. Schoon).

1387-3806/$ – see front matter © 2004 Elsevier B.V. All rights reserved.
doi:10.1016/j.ijms.2004.09.003

gas chromatography–mass spectrometry (GC–MS)[12,14] or gas chromatography with Fourier transform infrared spectroscopy (GC–FTIR) [12]. Vinckier et al. use a method based on sample collection on a liquid nitrogen trap followed by either the direct analysis by GC–MS [16] or a derivatization of the mono- and di-carbonyl compounds with 2-4-dinitrophenylhydrazine (DNPH). In the latter case, the chemical analysis was performed by high-performance liquid chromatography with mass spectrometric detection (HPLC–MS) [17]. Separation of gas and aerosol samples by use of suitable denuder/filter pack systems followed by GC–MS was applied by Yu et al. [18] and Jaoui and Kamens [19]. Also direct FTIR spectroscopy [9,20–22] has been used. Recently atmospheric pressure ionization (API) mass spectrometry [15,23,24] and proton transfer reaction mass spectrometry (PTR-MS) [25] have also been used to detect monoterpene oxidation products in laboratory studies.

Although in the last decade, considerable progress has been made in our understanding of the atmospheric oxidation processes of monoterpenes [26], a number of uncertainties still exist concerning the nature and yield of the different oxidation products. Therefore, continuous studies in this field are needed.

In a recent effort to apply chemical ionization mass spectrometry (CIMS) methods to the study of the monoterpene oxidation mechanisms, we have developed a new instrument, which consists of the coupling of a neutral fast flow reactor to a flowing afterglow instrument [27]. It is the intention to detect and quantify with this instrument the monoterpenes, as well as their oxidation products, as products of ion–molecule reactions with carefully chosen primary ions, such as H_3O^+, NO^+ or the open shell cation $O_2^{\bullet +}$ (further on simply noted as O_2^+). To do so, however, kinetic data (reaction rate constants) and information concerning the product distribution of the ion–molecule reactions involved are required.

For two of the major monoterpene oxidation products, acetone and formaldehyde, the reactions with H_3O^+, NO^+ and O_2^+ ions have been studied before [28], whereas only recently, studies of the reactions of these ions with the monoterpenes themselves have been reported [29,30].

For most monoterpene oxidation products, however, no such data are available. In the present work, we have studied the ion–molecule reactions of H_3O^+, NO^+ and O_2^+ with pinonaldehyde ($C_{10}H_{16}O_2$, a major oxidation product of α-pinene); nopinone ($C_9H_{14}O$, a major oxidation product of β-pinene), caronaldehyde ($C_{10}H_{16}O_2$, a major oxidation product of Δ^3-carene); 4-acetyl-1-methylcyclohexene ($C_9H_{14}O$, a major oxidation product of limonene) and α-pinene oxide ($C_{10}H_{16}O$, a minor oxidation product of α-pinene). A schematic representation of the structure of the products included in this study is given in Fig. 1.

Apart from giving the information required for our laboratory studies of monoterpene oxidation mechanisms, our present data also give information on the feasibility of using H_3O^+, NO^+ or O_2^+ as primary ions for in situ detection of monoterpene oxidation products through the selected ion flow tube–mass spectrometry (SIFT–MS) method, applied by Smith and co-workers for the measurement of a number of organic compounds [31–35].

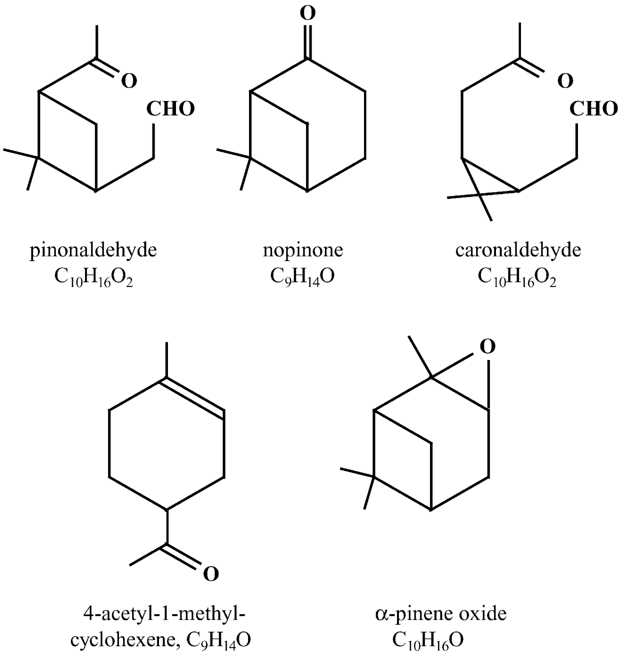

Fig. 1. Schematic representation of the monoterpene oxidation products studied.

2. Experimental

2.1. Instrumental

All measurements described here were performed at 1.5 mbar and 300 K with our SIFT, which is based upon the original design by Smith and Adams [36] and which has been described in detail previously [29]. Therefore, only a brief review of the instrument is given here.

The precursor ions are produced in a microwave discharge in a mixture of air and water vapor at a total pressure of 0.2 mbar. The ions are extracted from the discharge into a differentially pumped quadrupole mass spectrometer, where the appropriate ion (H_3O^+, NO^+ or O_2^+) is selected. The mass selected ions are then injected into the flow tube, where they are convectively transported by a main carrier helium gas flow. At the downstream end of the flow tube, the ions are sampled through a 0.4 mm hole, drilled into a conically shaped biased inlet flange into the analyzer quadrupole, where they are filtered according to their mass to charge ratio and detected by an electron multiplier, the signals of which are treated by pulse counting techniques.

Appropriate connections are foreseen at the flow tube for reactant gas and calibration gas inlet and pressure measurement.

2.2. Measurement methods

The ion–molecule reaction rate constant k is derived from the logarithmic decay $\ln(I/I_o) = -k\tau[X]$ of the source ion signal I versus the concentration of the reactant neutral $[X]$ in the flow tube. The residence time τ of the ions in the flow tube can be measured separately.

For the introduction of controlled amounts of the reactant gases into the flow tube, by means of a ring shaped inlet, located at 27 cm from the ion inlet plate of the analyzing quadrupole, different methods were used.

For 4-acetyl-1-methylcyclohexene, nopinone and α-pinene oxide the concentration of the reactant neutral was varied by flowing volumetric mixtures of the compound in helium, prepared in volume calibrated glass containers, into the flow tube through a needle valve heated at 315 K. From the pressure decay versus time in the glass container the gas flow could be determined and from the simultaneous measurements of the main carrier flow and pressure in the flow tube, the concentration $[X]$ of the reactant could be inferred. In this way, the reaction rate constants k of H_3O^+ with these three compounds could be determined absolutely. For each k measurement at least four different mixing ratios of the volumetric mixtures were used. The rate coefficients for the reactions with NO^+ and O_2^+ were then determined in a relative way, as described in a previous paper [29] and as used in previous studies by Španěl et al. [28].

For pinonaldehyde and caronaldehyde, however, the method of volumetric mixtures in helium could not be used, because of the low vapor pressure of these liquids [37]. In a first set of experiments with pinonaldehyde, a method has been used, which we originally developed for the introduction of methane sulfonic acid in the flow tube [38]. Pinonaldehyde was stored in a small glass reservoir, which was completely submerged in a water bath heated at 320 K. A flow of He, circulating through a spiral shaped copper tube, also submerged in the water bath, passed through the glass reservoir, where it was supposed to be saturated with pinonaldehyde vapor. Since the vapor pressure as a function of temperature is known [37] the concentration of the reactant $[X]$ can in this case be calculated from the He flow through the glass reservoir, the pressure in the glass reservoir, the main carrier flow and the pressure in the flow tube.

Unfortunately, this method led to irreproducible results, due to the very slow evaporation rate and the sticky nature of pinonaldehyde. In a second set of experiments a well-determined amount of liquid pinonaldehyde in a small stainless steel weighing boat was put into a cylindrical glass container of 5 l filled with helium. This container was then held at 360 K in a furnace, which also contained the pressure gauge. The glass cylinder was connected to the reactant gas inlet of the flow tube through a short heated stainless steel tube and a heated stainless steel needle valve. By choosing the amount of pinonaldehyde ($n = m/M$ with m = weight of pinonaldehyde in the weighing boat and M its molecular mass) in such a way that the pressure calculated from the ideal gas law ($p = nkT$) at $T = 360$ K is lower than the vapor pressure of pinonaldehyde at 360 K (9.7 mbar according to formula III of Hallquist et al. [37]), we can assume that all pinonaldehyde in the cylinder is in the gas phase. From the pressure decay in the glass cylinder with helium + pinonaldehyde we can then again derive the flow of reactant in the flow tube and thus the concentration $[X]$.

After the experiment, however, a brownish residue was remaining in the weighing boat, which represented in some cases up to 50% of the original quantity of pinonaldehyde. This could be due to polymerization of pinonaldehyde at elevated temperatures. Correcting for this weight residue we can only determine an upper limit for $[X]$, since we cannot exclude some deposition (and thus weight loss) of the pinonaldehyde or its polymer on other surfaces (glass reservoir, gas leads). As a result, the rate constant measured in this way is underestimated.

The same procedure was applied for caronaldehyde and the same problems were encountered. Our results for the rate coefficient of the reaction of H_3O^+ with pinonaldehyde and caronaldehyde are, therefore, lower limits.

Spectra of the reaction products recorded when pinonaldehyde and caronaldehyde were introduced with the cylinder/furnace method or with the method where helium is blown over the liquid at 320 K, result in the same reaction products.

The reaction rate coefficients for the reaction of NO^+ and O_2^+ with both keto-aldehydes were again determined in the usual relative way using the same reactant gas inlet method as for the absolute measurements with H_3O^+.

For the determination of the reaction product distribution a removable reactant gas inlet is used, which is located at 8 mm from the ion inlet plate to avoid diffusion enhancement effects [39]. 4-Acetyl-1-methylcyclohexene and nopinone were introduced using volumetrically prepared mixtures in helium and for α-pinene oxide, pinonaldehyde and caronaldehyde the method where helium is blown over the liquid was used.

Reaction product distributions were obtained using either the so-called scan mode or in the multi ion mode. In the scan mode a mass spectrum is obtained over a predetermined mass range by sweeping the ion mass spectrometer over the selected mass range. In the multi ion mode the mass spectrometer is switched sequentially at a number of fixed masses (maximum 20 in our case) and the count rate at those masses is measured.

To eliminate mass discrimination effects regular measurements with calibration gases were performed, as described earlier [29].

2.3. Chemicals

Nopinone and α-pinene oxide, obtained commercially from Aldrich, were 98 and 97% pure, respectively. The compound 4-acetyl-1-methylcyclohexene was a “library product” of Sigma Aldrich and was sold “as is” (no purity specified). Pinonaldehyde and caronaldehyde were synthesized by ozonolysis of the corresponding monoterpene (α-pinene and Δ^3-carene) [16,40]. Their purity, as deduced from the GC–MS analysis, is estimated to be 98% for batch 1 of pinonaldehyde, 95% for batch 2 of pinonaldehyde and 95% for caronaldehyde. The He carrier gas (Air Products) was BIP quality (99.9995%). To quench possible excited precursor ions a small amount of N_2 (Air Products, 6.0 quality, 99.9999%) was added to the carrier gas.

3. Results

3.1. *Ion–molecule reaction rate coefficient and quantum mechanical calculations*

The experimentally derived values for the reaction rate constant k_{exp} for the H_3O^+, NO^+ and $O_2{}^+$ reactions with the five monoterpene oxidation products are shown in Table 1.

As explained in Section 2, the k_{exp} values for the H_3O^+ reactions with 4-acetyl-1-methylcyclohexene, nopinone and α-pinene oxide were derived in an absolute way from the decay of the source ion signal versus the reactant concentration, inferred from absolute flow rates, which were obtained by monitoring the pressure decrease of the reactant/helium mixture, prepared volumetrically at room temperature. The reaction rate constants for the NO^+ and $O_2{}^+$ reactions were measured relatively with respect to the one of H_3O^+ by recording the decay of the three source ions simultaneously (or subsequently) with increasing concentration of the reactant, introduced into the flow tube via a flowmeter/controller.

For pinonaldehyde and caronaldehyde the same procedure was used, but the reactant gas mixture was obtained by heating a well-defined weight of liquid in a glass bottle filled with helium. For reasons, explained before, this method only resulted in a lower limit of the reaction rate constants.

The accuracy of the experimental rate constants shown in Table 1 is estimated to be 25% with a precision better than 5% for the relative measurements, about 5% precision for the absolute measurements with 4-acetyl-1-methylcyclohexene and α-pinene oxide and 15% precision for the absolute measurements with nopinone, pinonaldehyde and caronaldehyde.

It is customary to compare the experimental results with the collision rate constants k_C, calculated with the parameterized equation of Su and Chesnavich [41,42], based upon trajectory calculations:

$$k_C = k_L C(\alpha, \mu_D, T), \tag{1}$$

where C is a parameterized equation, depending upon α, μ_D and temperature T; α and μ_D are the polarizability and the dipole moment of the ion.

The Langevin rate constant k_L is given by the formula:

$$k_L = 2\pi q\sqrt{\frac{\alpha}{\mu}}, \tag{2}$$

where q is the absolute value of the charge of the ion, and μ the reduced mass of the ion–molecule system (all variables in atomic units).

As far as we know, no information is available for the dipole moment and polarizability of the monoterpene oxidation products studied here. The values for α and μ_D, which allow us to evaluate k_C, were, therefore, obtained by quantum chemical calculations using the Gaussian software suite [43]. As the off-diagonal elements of the polarization matrix are small in all cases, the overall polarizability α was derived by averaging the α_{XX}, α_{YY} and α_{ZZ} polarizabilities.

An additional complexity with three of the five compounds studied here (4-acetyl-1-methylcyclohexene, pinonaldehyde and caronaldehyde) is the existence of multiple rotameric forms, i.e. different orientations of the polar substituents due to internal rotations along single bonds, and for one compound, α-pinene oxide, the occurrence of geometric (syn/anti) isomerism.

For nopinone, and for α-pinene oxide in either its syn or anti form, i.e. all structures without internal rotations affecting the dipole moment or polarizability, we calculated α and μ_D at the B3LYP-DFT level of theory using the large aug-cc-pVDZ basis set.

For 4-acetyl-1-methylcyclohexene six rotamers exist, each with a different value of α and μ_D, while for caronaldehyde we located 44 rotamers and for pinonaldehyde 27. For all these rotamers α and μ_D were calculated using B3LYP-DFT/6-31G(d,p). In addition, for the thermally most populated rotamers of these three compounds, the calculations were refined at the higher B3LYP-DFT/aug-cc-pVDZ level of theory. For 4-acetyl-1-methylcyclohexene, the two most abundant rotamers constitute 90% of the population, while for caronaldehyde the eight most populated rotamers cover

Table 1
Polarizability, dipole moment and reaction rate constants of the monoterpene oxidation products

Molecule	α (Å^3)	μ_D (Debye)	$k_{\text{exp}}[k_C]$ (H_3O^+)	k_{exp} $[k_C]$ (NO^+)	k_{exp} $[k_C]$ ($O_2{}^+$)
4-Acetyl-1-methyl-cyclohexene	16.3	2.90	4.2 [4.2]	3.7 [3.4]	3.6 [3.4]
Nopinone	15.7	3.50	4.2 [4.7]	3.8 [3.9]	3.7 [3.8]
α-Pinene oxide[a]	17.3	1.99	3.3 [3.4]	2.9 [2.8]	2.8 [2.7]
Pinonaldehyde	17.9	2.26	≥2.7 [3.8]	≥2.3 [3.1]	≥2.3 [3.0]
Caronaldehyde	18.1	3.58	≥4.0 [4.9]	≥3.3 [4.0]	≥3.8 [3.9]

Polarizability α and dipole moment μ_D of the monoterpene oxidation products at 300 K, obtained from quantum chemical calculations. Experimentally determined rate constants k_{exp} for the reactions of H_3O^+, NO^+ and $O_2{}^+$ with the five monoterpene oxidation products and in square brackets their corresponding collisional rate constants k_C, calculated with the parameterized equation of Su and Chesnavich. Rate constants are expressed in 10^{-9} molecule^{-1} cm^3 s^{-1}.

[a] Since the values of α, μ_D and k_C for α-pinene oxide in its syn or anti-configuration only differ slightly, the averaged values of these parameters are listed.

74% and for pinonaldehyde the four most abundant rotamers span 75% of the population. The values of α and μ_D shown in Table 1 were then obtained by calculating for each compound the thermally weighted average of the α and μ_D values over the different rotamers, using the B3LYP/aug-cc-pVDZ value where available, and B3LYP/6-31G(d,p) values elsewhere. Similarly, the value of k_C in Table 1 is the thermally weighted average of the reaction rate constants, calculated for each rotamer separately. To assess the impact on the predicted k_C of incorporating the less accurate B3LYP/6-31G(d,p) data instead of B3LYP/aug-cc-pVDZ results for the least populated rotamers, we compared the systematic change between the two levels of theory. We found that, in general, moving from B3LYP/6-31G(d,p) to B3LYP/aug-cc-pVDZ results in an increase of the polarizability α of the rotamer of 20%, whereas the dipole moment μ_D increases or decreases by at most 15%. By replacing the B3LYP-DFT/6-31G(d,p) polarizabilities α_L and the dipole moments μ_{DL} for the less populated rotamers by $1.2 \times \alpha_L$ and $0.8 \times \mu_{DL}$ or $1.2 \times \mu_{DL}$ in the calculation of k_C, a change of at most 7% was found for the predicted value of k_C. We, therefore, believe that the uncertainty on k_C, induced by using B3LYP/6-31G(d,p) instead of B3LYP/aug-cc-pVDZ values for the least populated rotamers, is at most 10%.

As is noticed from Table 1, the reactions of 4-acetyl-1-methylcylohexene, nopinone and α-pinene oxide with H_3O^+, NO^+ and $O_2{}^+$ proceed within the experimental error at the collision rate.

For the reactions of pinonaldehyde and caronaldehyde no unambiguous conclusion can be drawn, since only lower limits were obtained for the reaction rate constants. However, several studies have shown that for exothermic proton transfer reactions, as we are dealing with here (see further on), k always equals k_C. It is, therefore, plausible to assume that this is also the case for the reaction of H_3O^+ with pinonaldehyde and caronaldehyde. Moreover, the fact that the ratio $k_{exp}(NO^+)/k_{exp}(H_3O^+)$ equals $k_C(NO^+)/k_C(H_3O^+)$ within the experimental error for both compounds, suggests that the reactions of pinonaldehyde and caronaldehyde with H_3O^+ and NO^+ proceed at the collision rate. The same goes for the reaction of $O_2{}^+$ with pinonaldehyde.

The reaction of caronaldehyde with $O_2{}^+$, however, proceeds as fast as the reaction with H_3O^+ (see Table 1), whereas theory predicts $k_C(O_2{}^+) = 0.8\ k_C(H_3O^+)$. Therefore, in the very plausible assumption that H_3O^+ reacts with caronaldehyde at the collision rate and based upon the relative measurement of the reaction rate constant of $O_2{}^+$ versus the one of H_3O^+, the reaction rate constant for $O_2{}^+$ should then equal 4.7×10^{-9} molecule^{-1} cm^3 s^{-1}, which exceeds the corresponding collisional rate constant by 20%. Although for charge transfer processes this cannot be excluded, due to possible long range resonant electron transfer, that happens at intermolecular distance larger than the critical distance for the formation of a Langevin reaction complex and which is not considered in the Su and Chesnavich theory, it is not clear why this happens only in the case of the $O_2{}^+$–caronaldehyde reaction.

Three-body association channels have been observed for the reactions of NO^+ with nopinone and caronaldehyde (see Table 2 hereafter). However, their fraction is too small to conclude whether the effective bimolecular rate constant of these association channels equals their high-pressure limit under our experimental conditions.

3.2. Product distributions

The branching ratios of the different product ions of the reactions of H_3O^+, NO^+ and $O_2{}^+$ with the five oxidation products of monoterpenes are listed in Table 2.

A glance at this table already reveals the complexity of the chemistry involved in the major part of these reactions. Therefore, and since no thermodynamical data about these products are available, only the major reaction channels will be discussed.

3.2.1. H_3O^+ reactions

All H_3O^+ reactions with the reactants M proceed through proton transfer, indicating that the proton affinity of these reactants is larger than the one of H_2O (691 kJ/mol [44]). In the case of 4-acetyl-1-methylcyclohexene and nopinone this transfer is mainly non-dissociative, resulting in one major product, the protonated reactant MH^+:

$$M + H_3O^+ \rightarrow MH^+ + H_2O. \qquad (3)$$

In this respect, our results for 4-acetyl-1-methylcyclohexene and nopinone confirm the observations of Španěl et al. [28], who found that the reactions of H_3O^+ with a number of ketones, including the cyclic non-aromatic menthone, proceed via proton transfer and produce only the protonated ketone under SIFT conditions.

Wisthaler et al. [25] have used the reaction of H_3O^+ with nopinone for the detection of this compound by PTR-MS. From this work it turns out that under PTR-MS conditions, next to the protonated nopinone cation, elimination of a water molecule is distinctly observed, as well as minor products at $m/z = 83$ and 93. The difference between these results and the data reported here can most likely be explained by the enhanced energy of the precursor ions, due to the applied electric field in the drift tube of the PTR-MS experiment, which can lead to an enhanced break-up of the protonated molecule.

Such enhanced break-up has also been observed in atmospheric pressure chemical ionization spectra of nopinone and ion trap MS spectra of protonated nopinone [46], which also clearly show the H_2O abstraction from protonated nopinone and the minor product at $m/z = 83$.

For α-pinene oxide, pinonaldehyde and caronaldehyde the proton transfer reaction is dissociative, even under SIFT conditions, resulting in a series of fragments of the nascent ex-

Table 2
Product ion distribution[a] of the reactions of H_3O^+, NO^+ and O_2^+ with 4-acetyl-1-methylcyclohexene, nopinone, α-pinene oxide, pinonaldehyde and caronaldehyde at 1.5 mbar and 300 K

Molecule	H_3O^+			NO^+			O_2^+		
	m/z	Product ion	%	*m/z*	Product ion	%	*m/z*	Product ion	%
4-Acetyl-1-methyl-Cyclohexene $C_9H_{14}O$ *m* = 138 u	139	$C_9H_{15}O^+$	89	137	$C_9H_{13}O^+$	2	80		2
	140	$C_9H_{15}O^{+,b}$	9	138	$C_9H_{14}O^+$	85	94		4
	Others		2	139	$C_9H_{14}O^{+,b}$	9	95		16
				Others		4	96		2
							120	$C_9H_{12}^+$	2
							123	$C_8H_{11}O^+$	12
							124	$C_8H_{11}O^{+,b}$	1
							138	$C_9H_{14}O^+$	48
							139	$C_9H_{14}O^{+,b}$	6
							Others		7
Nopinone $C_9H_{14}O$ *m* = 138 u	139	$C_9H_{15}O^+$	88	127		4	82		3
	140	$C_9H_{15}O^{+,b}$	9	138	$C_9H_{14}O^+$	60	83		15
	Others		3	139	$C_9H_{14}O^{+,b}$	7	84		1
				168	$(NO\cdot C_9H_{14}O)^+$	17	95		5
				169	$(NO\cdot C_9H_{14}O)^{+,b}$	2	96		9
				Others		10	97		3
							109		9
							110		5
							120	$C_9H_{12}^+$	2
							123	$C_8H_{11}O^+$	5
							138	$C_9H_{14}O^+$	30
							139	$C_9H_{14}O^{+,b}$	5
							Others		8
α-Pinene oxide $C_{10}H_{16}O$ *m* = 152 u	43		2	94		4	82		9
	93		9	108		10	83		7
	95		2	109		7	84		2
	107		2	110		16	94		4
	109	$C_7H_9O^{+,c}$	14	111		2	95		4
	110	$C_7H_9O^{+,b,c}$	1	123		3	96		2
	135	$C_{10}H_{15}^+$	47	134	$C_{10}H_{14}^+$	8	108		3
	136	$C_{10}H_{15}^{+,b}$	5	135	$C_{10}H_{14}^{+,b}$+ Other product	3	109		19
	153	$C_{10}H_{17}O^+$	10				110		3
	154	$C_{10}H_{17}O^{+,b}$	1	137	$C_9H_{13}O^+$	6	134	$C_{10}H_{14}^+$	2
	Others		7	151	$C_{10}H_{15}O^+$	3	137	$C_9H_{13}O^+$	19
				152	$C_{10}H_{16}O^+$	24	138	$C_9H_{13}O^{+,b}$	2
				153	$C_{10}H_{16}O^{+,b}$	3	152	$C_{10}H_{16}O^+$	10
				Others		11	153	$C_{10}H_{16}O^{+,b}$	1
							Others		13
Pinonaldehyde $C_{10}H_{16}O_2$ *m* = 168 u	61		2	97		12	71		3
	71	$C_4H_7O^{+,e}$	4	98		3	82		8
	93		2	99		13	83		4
	99		5	100		2	97		14
	107	$C_8H_{11}^{+,d}$	9	124		2	98		21
	123		2	140		18	99		3
	151	$C_{10}H_{15}O^+$	54	141		3	107		2
	152	$C_{10}H_{15}O^{+,b}$	6	150	$C_{10}H_{14}O^+$	3	108		2
	169	$C_{10}H_{17}O_2^+$	7	167	$C_{10}H_{15}O_2^+$	18	109		3
	Others		9	168	$C_{10}H_{16}O_2^+$ $C_{10}H_{15}O_2^{+,b}$	12	111		3
							124		6
				169	$C_{10}H_{16}O_2^{+,b}$	3	125		4
				Others		11	140		8
							168	$C_{10}H_{16}O_2^+$	3
							Others		16
Caronaldehyde $C_{10}H_{16}O_2$ *m* = 168 u	61		3	43		3	43		2
	93		3	69		2	82		3
	107	$C_8H_{11}^{+,f}$	10	97		4	83		2
	108	$C_8H_{11}^{+,b,f}$	1	110		2	84		8
	109	$C_8H_{13}^{+,f}$	4	111		6	86		4

Table 2 (*Continued*)

Molecule	H_3O^+			NO^+			O_2^+		
	m/*z*	Product ion	%	*m*/*z*	Product ion	%	*m*/*z*	Product ion	%
	123		18	112		2	97		2
	124		2	124		3	107		2
	125		2	125		4	108		3
	133		2	126		2	110		3
	139		2	138		4	111		14
	141		2	139		3	112		2
	151	$C_{10}H_{15}O^+$	20	140		10	122		2
	152	$C_{10}H_{15}O^{+,b}$	2	141		1	124		4
	167	$C_{10}H_{15}O_2^+$	2	152		2	125		7
	169	$C_{10}H_{17}O_2^+$	12	167	$C_{10}H_{15}O_2^+$	3	139		11
	170	$C_{10}H_{17}O_2^{+,b}$	1	168	$C_{10}H_{16}O_2^+$	11	140		4
	Others		14	169	$C_{10}H_{16}O_2^{+,b}$	2	168	$C_{10}H_{16}O_2^+$	3
				180	$(NO.C_{10}H_{14}O)^+$	8	169	$C_{10}H_{16}O_2^{+,b}$	1
				181	$(NO.C_{10}H_{14}O)^{+,b}$	1	Others		23
				198	$(NO.C_{10}H_{16}O_2)^+$	4			
				Others		23			

[a] Only products with branching ratio ≥2% are listed. Products with smaller branching ratio's are grouped together in "others", with exception of products at *m*/*z* with branching ratio between 1 and 2%, which are clearly the ^{13}C-isotope of the products at $(m-1)/z$.

[b] ^{13}C-isotope.

[c] Tentative product identification.

[d] Product identification according to Ref. [46].

[e] Product identification according to Ref. [25].

[f] In analogy with pinonaldehyde, product identification for pinonaldehyde according to Ref. [46].

cited protonated reactant $(MH^+)^*$. The protonated reactant MH^+ is still one of the major products, but the dominating channel is elimination of a water molecule after protonation, resulting in the $(M-OH)^+$ cation:

$$M + H_3O^+ \rightarrow (M-OH)^+ + 2H_2O. \tag{4}$$

For pinonaldehyde and caronaldehyde, which are both keto-aldehydes, this fits well within the results of the SIFT study of the reaction of H_3O^+ with a series of aldehydes by Španěl et al. [28,45], who observed, next to the protonated aldehyde, H_2O elimination after protonation for saturated aldehydes with at least four carbon atoms (except 2-methylpropanal).

Water abstraction from protonated pinonaldehyde was also confirmed by ion trap MS spectra, reported by Warscheid [46].

Apart from the minor ions at $m/z = 93$ and $m/z = 61$, all the products of the H_3O^+–pinonaldehyde reaction shown in Table 2, were also observed in a PTR-MS study by Wisthaler et al. [25]. In addition these authors also detect mass 81, which we do not see. Furthermore, the smaller fragments all occur with a larger abundance in the PTR-MS experiment, indicating again a higher break-up in PTR-MS than under SIFT–MS conditions.

The product observed at $m/z = 107$ for pinonaldehyde has also been detected by Warscheid [46] and has been explained by simultaneous or subsequent ejection of H_2O and C_2H_3OH. Mass 109 observed by this author was assigned to the loss of H_2O and H_2C_2O from protonated pinonaldehyde.

Next to the products due to protonation and subsequent water abstraction, other non-negligible products are observed at $m/z = 109$ for the H_3O^+–α-pinene oxide reaction, and at $m/z = 107$ and 123 for caronaldehyde.

In the cases where many fragment ions were observed, the reactant was introduced in the flow tube by flowing He (typically 1.7 STP $cm^3\,s^{-1}$) over the liquid reactant, stored in a reservoir (heated at 320–330 K in the case of pinonaldehyde and caronaldehyde). During the measurements of the product distribution of the H_3O^+–caronaldehyde reaction the relative intensity of the fragments at $m/z = 61$, 139 and 167 (all fragments with branching ratio ≤3%) increased, which could indicate that these ions (or a fraction of them) originate from impurities, which have a larger evaporation rate than caronaldehyde. Therefore, the branching ratio of these fragments should be taken with some reservation.

3.2.2. NO^+ reactions

In all the reactions of NO^+ with the five monoterpene oxidation products charge transfer occurs, indicating that the ionization energy of these reactants is smaller than the one of NO (9.26 eV [44]):

$$M + NO^+ \rightarrow M^+ + NO. \tag{5}$$

For 4-acetyl-1-methylcyclohexene, nopinone and α-pinene oxide the parent cation is clearly the most abundant ion (94, 67 and 27%, respectively). The charge transfer process is highly dissociative in the reactions with α-pinene oxide, pinonaldehyde and caronaldehyde, resulting in several fragments of the nascent excited $(M^+)^*$ cation. Elimination of H_2O, for instance, occurs for the NO^+–α-pinene oxide and pinonaldehyde reactions, resulting in a product at $m/z = 134$ and 150, respectively. Another example is the ejection of

C_2H_4 (or CO), as observed in many charge transfer reactions of O_2^+ with aldehydes [28,45], giving the product at $m/z = 140$ in the NO^+–pinonaldehyde and caronaldehyde reactions.

For pinonaldehyde one of the dominant pathways is hydride ion transfer:

$$M + NO^+ \rightarrow (M - H)^+ + HNO, \tag{6}$$

a process, which has also been observed by Španěl et al. in their study of the NO^+ reaction with a series of aldehydes [28,45] (even the only reaction pathway for the saturated aldehydes they have studied) and with a series of alcohols [47]. H^--transfer is also a reaction channel, although minor, in the reaction of NO^+ with 4-acetyl-1-methylcyclohexene, α-pinene oxide and caronaldehyde.

A third reaction pathway, three-body association, is observed in the reaction of NO^+ with nopinone and caronaldehyde:

$$M + NO^+ + He \rightarrow (M \cdot NO)^+ + He, \tag{7}$$

(for caronaldehyde the mass discrimination factor for the product at $m/z = 198$ was obtained through extrapolation of the curve fitted through measured mass discrimination factors at lower m/z values [29], which implies a larger error on the branching ratio of this association product).

Remarkable is the product at $m/z = 180$ in the NO^+–caronaldehyde reaction, the branching ratio of which is too high to be attributed to impurities. This product can only result from fragmentation of the excited association complex $(M{\cdot}NO)^{+*}$ through H_2O ejection. Similarly, the minor product at $m/z = 127$ in the NO^+–nopinone reaction can only originate from fragmentation of the association product.

The branching ratio for the product at $m/z = 125$ in the NO^+–caronaldehyde reaction is somewhat uncertain due to the role of possible evaporating impurities, as explained at the end of Section 3.2.1.

3.2.3. O_2^+ reactions

All O_2^+ reactions can be classified as charge transfer reactions. This is quite evident in view of the previous section, since the ionization energy of O_2 exceeds the one of NO by about 3 eV.

For the reaction of O_2^+ with 4-acetyl-1-methylcyclohexene and nopinone the parent cation remains the major product, while for pinonaldehyde and caronaldehyde it is only a minor product. In all cases, the charge transfer process is sufficiently exothermic to result in significant cracking of the nascent excited parent cations $(M^+)^*$. For example, we observe the elimination of a H_2O molecule for all reactions (for pinonaldehyde and caronaldehyde < 2%), and the ejection of the alkyl radical CH_3 for the reactions of O_2^+ with 4-acetyl-1-methylcyclohexene, nopinone and α-pinene oxide.

Many O_2^+–SIFT studies have shown that generally the greater the atomicity of the reactant, the more fragments are observed, a feature often mirrored in the corresponding electron impact (EI) spectra.

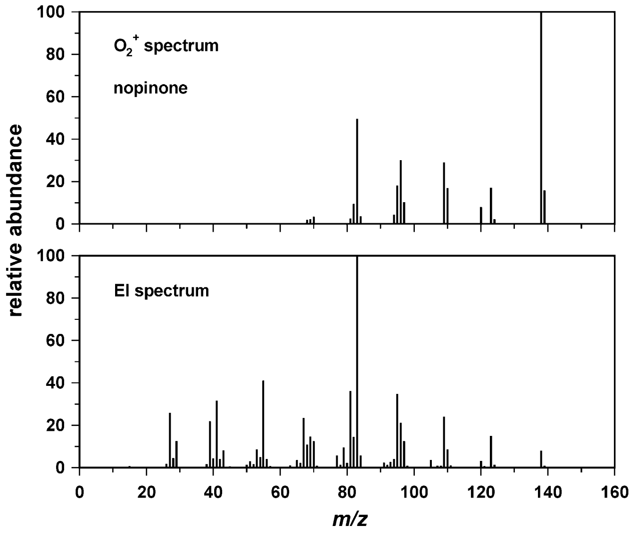

Fig. 2. Comparison between the O_2^+ spectrum of nopinone with its corresponding EI spectrum [44].

It is clear that the O_2^+ reactions with α-pinene oxide, pinonaldehyde and caronaldehyde are not very well suited for the identification and the quantification of these monoterpene oxidation products, due to the extensive fragmentation.

Figs. 2 and 3 show the comparison between the O_2^+ spectrum for nopinone and α-pinene oxide with their corresponding EI spectrum (70 eV) [44].

Although all the products observed in the SIFT–MS spectra can also be identified in the EI spectra, the latter show much more fragmentation and a more pronounced relative intensity of the smaller fragments, since O_2^+ reaction is a “softer” ionization technique than EI.

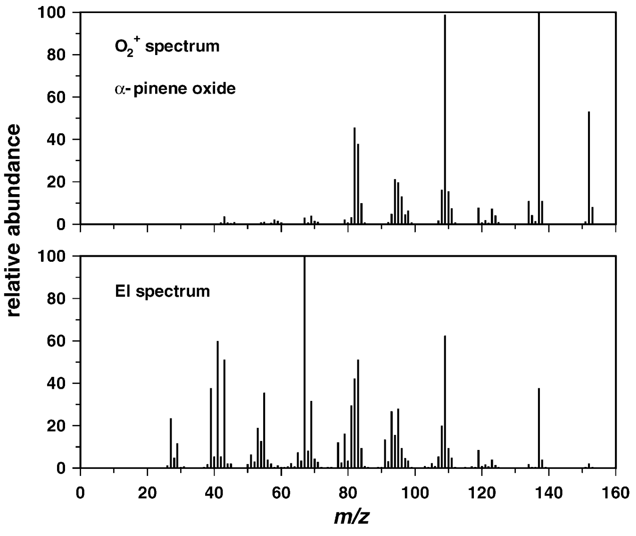

Fig. 3. Comparison between the O_2^+ spectrum of α-pinene oxide with its corresponding EI spectrum [44].

Comparison of the EI spectrum of pinonaldehyde, recorded by Jaoui and Kamens [19], with the corresponding O_2^+ spectrum confirm the previous remarks. In the first the major product ions are at $m/z = 43$, 69 and 83.

4. Concluding remarks

It has been shown that the reactions of H_3O^+, NO^+ and O_2^+ with the five monoterpene oxidation products are fast and that their reaction rates are close to the collision rate constant, derived from the Su–Chesnavich formula and extensive quantum chemical calculations of the dipole moment and polarizability of these reactants.

Based upon the results described in Section 3.2, we can conclude that for experiments, where only one monoterpene oxidation product is present, H_3O^+ is the most suited precursor ion to quantify the product, based upon the protonated reactant at $m/z = 139$ for 4-acetyl-1-methylcyclohexene and nopinone, and upon the (protonated reactant—H_2O) at $m/z = 135$, 151 and151 for α-pinene oxide, pinonaldehyde and caronaldehyde, respectively.

However, if mixtures of the structural isomers nopinone and 4-acetyl-1-methylcyclohexene, or of the isomers pinonaldehyde and caronaldehyde are present, H_3O^+ is not suitable, since the product distributions of the reactions of these isomers with H_3O^+ are quite similar. Only when an averaged rate constant and an averaged product distribution are used, an estimation of the concentration of the mixture can be obtained.

However, in this case NO^+ can be used as a precursor ion to quantify the reactants separately, since nopinone and caronaldehyde distinctly associate in their reaction with NO^+, whereas their structural isomers 4-acetyl-1-methylcyclohexene and pinonaldehyde, respectively, do not (branching ratio <1%).

Similarly, O_2^+ primary ions are suitable to distinct the nopinone and 4-acetyl-1-methylcyclohexene isomers, based upon the product at $m/z = 83$, or upon $m/z = 98$ for the isomeric pair pinonaldehyde-caronaldehyde.

It should be stressed that, especially for pinonaldehyde and caronaldehyde, a very large number of fragments with branching ratio <2% were observed, which is reflected in the large value for “others” in Table 2. On the other hand, when using different sample preparations for caronaldehyde, some variation in the relative intensity of minor reaction products is observed, which could indicate that some of these minor products are (partially) due to impurities. Therefore, products with small branching ratios should be taken with some reservation and it is not excluded that the values of “others” (see Table 2) is somewhat overestimated. The above mentioned remark accounts also, although to lesser extent, for pinonaldehyde.

As already mentioned in previous work [29], if product distributions are used to quantify the concentration of reactants by chemical ionization, the product distribution has to be determined under the same CIMS conditions (carrier gas, pressure in the flow tube, voltage on the inlet plate of the detector quadrupole, ...).

Acknowledgements

This work was partly funded by the Belgian “Federal Office for Scientific, Technical and Cultural Affairs” within the framework of the “Scientific support plan for a sustainable development policy (SPSD 2)—Global change, ecosystems and biodiversity—Project EV/35/06”.

References

[1] B. Lamb, A. Guenther, D. Gay, H. Westberg, Atmos. Environ. 21 (1987) 1695.
[2] J.-F. Müller, J. Geophys. Res. 97 (1992) 3787.
[3] A. Guenther, P. Zimmerman, M. Wildermuth, Atmos. Environ. 28 (1994) 1197.
[4] C. Geron, R. Rasmussen, R.R. Arnts, A. Guenther, Atmos. Environ. 34 (2000) 1761.
[5] R. Janson, K. Rosman, A. Karlsson, H.-C. Hansson, Tellus 53B (2001) 423.
[6] A. Guenther, C.N. Hewitt, D. Erickson, R. Fall, C. Geron, T. Graedel, P. Harley, L. Klinger, M. Lerdau, W.A. McKay, T. Pierce, B. Scholes, R. Steinbrecher, R. Tallamraju, J. Taylor, P. Zimmerman, J. Geophys. Res. 100 (1995) 8873.
[7] B.R. Larsen, D. Di Bella, M. Glasius, R. Winterhalter, N.R. Jensen, J. Hjorth, J. Atmos. Chem. 38 (2001) 231.
[8] A. Römpp, B. Bonn, G.K. Moortgat, R. Winterhalter, R. Van Dingenen, M. Spittler, K. Wirtz, Proceedings of the Eighth European Symposium on the Physico-Chemical Behaviour of Atmospheric Pollutants, 17–20 September 2001, Torino, Italy, extended abstract TP24, CD ROM, 2002.
[9] J.J. Orlando, B. Nozière, G.S. Tyndall, G.E. Orzechowska, S.E. Paulson, Y. Rudich, J. Geophys. Res. 105 (2000) 11561.
[10] J. Arey, R. Atkinson, S.M. Aschmann, J. Geophys. Res. 95 (1990) 18539.
[11] H. Hakola, J. Arey, S.M. Aschmann, R. Atkinson, J. Atmos. Chem. 18 (1994) 75.
[12] A. Alvarado, E.C. Tuazon, S.M. Aschmann, R. Atkinson, J. Arey, J. Geophys. Res. 103 (1998) 25541.
[13] S.M. Aschmann, A. Reissell, R. Atkinson, J. Arey, J. Geophys. Res. 103 (1998) 25553.
[14] A. Reissell, C. Harry, S.M. Aschmann, R. Atkinson, J. Arey, J. Geophys. Res. 104 (1999) 13869.
[15] S.M. Aschmann, R. Atkinson, J. Arey, J. Geophys. Res. 107 (2002) D14, doi:10.1029/2001JD001098. ACH 6-1.
[16] C. Vinckier, F. Compernolle, A.M. Saleh, Bull. Soc. Chim. Belg. 106 (1997) 501.
[17] V. Van den Bergh, H. Coeckelberghs, H. Vankerckhoven, F. Compernolle, C. Vinckier, Anal. Bioanal. Chem. 379 (2004) 484.
[18] J. Yu, D.R. Cocker III, R.J. Griffin, R.C. Flagan, J.H. Seinfeld, J. Atmos. Chem. 34 (1999) 207.
[19] M. Jaoui, R.M. Kamens, J. Atmos. Chem. 44 (2003) 259.
[20] S. Hatakeyama, K. Izumi, T. Fukuyama, H. Akimoto, J. Geophys. Res. 94 (1989) 13013.
[21] S. Hatakeyama, K. Izumi, T. Fukuyama, H. Akimoto, N. Washida, J. Geophys. Res. 96 (1991) 947.
[22] B. Nozière, I. Barnes, K.-H. Becker, J. Geophys. Res. 104 (1999) 23645.

[23] B. Warscheid, T. Hoffmann, Rapid Commun. Mass Spectrom. 15 (2001) 2259.

[24] B. Warscheid, T. Hoffmann, Rapid Commun. Mass Spectrom. 16 (2002) 496.

[25] A. Wisthaler, N.R. Jensen, R. Winterhalter, W. Lindinger, J. Hjorth, Atmos. Environ. 35 (2001) 6181.

[26] R. Atkinson, J. Arey, Atmos. Environ. 37 (Suppl. 2) (2003) S197.

[27] C. Amelynck, N. Schoon, J. Riondato, E. Arijs, Geophysical Research Abstracts 5, EGS-AGU-EUG Joint Assembly, 6–11 April 2003. Nice, France, abstract number EAE03-A-02664 CD ROM.

[28] P. Španěl, Y. Ji, D. Smith, Int. J. Mass Spectrom. Ion Processes 165/166 (1997) 25.

[29] N. Schoon, C. Amelynck, L. Vereecken, E. Arijs, Int. J. Mass Spectrom. 229 (2003) 213.

[30] T. Wang, P. Španěl, D. Smith, Int. J. Mass Spectrom. 228 (2003) 117.

[31] P. Španěl, D. Smith, Med. Biol. Eng. Comput. 34 (1996) 409.

[32] D. Smith, P. Španěl, J.M. Thompson, B. Rajan, J. Cocker, P. Rolfe, Appl. Occup. Environ. Hyg. 13 (1998) 817.

[33] P. Španěl, S. Davies, D. Smith, Rapid Commun. Mass Spectrom. 13 (1999) 1733.

[34] P. Španěl, A.M. Diskin, S.M. Abbott, T. Wang, D. Smith, Rapid Commun. Mass Spectrom. 16 (2002) 2148.

[35] S.M. Abbott, J.B. Elder, P. Španěl, D. Smith, Int. J. Mass Spectrom. 228 (2003) 655.

[36] D. Smith, N.G. Adams, Adv. Atom. Mol. Phys. 24 (1988) 1.

[37] M. Hallquist, I. Wängberg, E. Ljungström, Environ. Sci. Technol. 31 (1997) 3166.

[38] N. Schoon, C. Amelynck, P. Bultinck, E. Arijs, Int. J. Mass Spectrom. 221 (2002) 209.

[39] P. Španěl, D. Smith, J. Am. Soc. Mass Spectrom. 12 (2001) 863.

[40] V. Rautenstrauch, B. Willhalm, W. Tommen, G. Ohloff, Helv. Chim. Acta 67 (1984) 325.

[41] T. Su, W.J. Chesnavich, J. Chem. Phys. 76 (1982) 5183.

[42] T. Su, J. Chem. Phys. 89 (1988) 5355.

[43] M.J. Frisch, G.W. Trucks, H.B. Schlegel, G.E. Scuseria, M.A Robb, J.R. Cheeseman, V.G. Zakrzewski, J.A. Montgomery Jr., R.E. Stratmann, J.C. Burant, S. Dapprich, J.M. Millam, A.D. Daniels, K.N. Kudin, M.C. Strain, O. Farkas, J. Tomasi, V. Barone, M. Cossi, R. Cammi, B. Mennucci, C. Pomelli, C. Adamo, S. Clifford, J. Ochterski, G.A. Petersson, P.Y. Ayala, Q. Cui, K. Morokuma, D.K. Malick, A.D. Rabuck, K. Raghavachari, J.B. Foresman, J. Cioslowski, J.V. Ortiz, A.G. Baboul, B.B. Stefanov, G. Liu, A. Liashenko, P. Piskorz, I. Komaromi, R. Gomperts, R.L. Martin, D.J. Fox, T. Keith, M.A. Al-Laham, C.Y. Peng, A. Nanayakkara, C. Gonzalez, M. Challacombe, P.M.W. Gill, B. Johnson, W. Chen, M.W. Wong, J.L. Andres, C. Gonzalez, M. Head-Gordon, E.S. Replogle, J.A. Pople, Gaussian 98, Revision A.7, Gaussian Inc., Pittsburgh PA, 1998.

[44] P.J. Linstrom, W.G. Mallard (Eds.), NIST Chemistry Webbook, NIST Standard Reference Database Number 69, March 2003, National Institute of Standards and Technology, Gaithersburg, MD 20899, USA (http://webbook.nist.gov);
E.P. Hunter, S.G. Lias, NIST Chemistry Webbook, NIST Standard Reference Database Number 69, March 2003, National Institute of Standards and Technology, Gaithersburg, MD 20899, USA (http://webbook.nist.gov);
S.G. Lias, NIST Chemistry Webbook, NIST Standard Reference Database Number 69, March 2003, National Institute of Standards and Technology, Gaithersburg, MD 20899, USA (http://webbook.nist.gov);
S.E. Stein, NIST Chemistry Webbook, NIST Standard Reference Database Number 69, March 2003, National Institute of Standards and Technology, Gaithersburg, MD 20899, USA (http://webbook.nist.gov).

[45] P. Španěl, J.M. Van Doren, D. Smith, Int. J. Mass Spectrom. 213 (2002) 163.

[46] B. Warscheid, dissertationsschrift, University of Dortmund.

[47] P. Španěl, D. Smith, Int. J. Mass Spectrom. Ion Processes 167/168 (1997) 375.